Article ID: #99201122. Received: July 31, 2021. Revised: August 31, 2021. Accepted: December 25, 2021

Journal of Bioinformatics and Neuroscience (JBINS), 7 (2): 328-333, December 31, 2021
e-ISSN: 2432-5422, p-ISSN: 2188-8116
Applied Science and Computer Science Publications

Geometric Shape Statistical Analysis of Tibial Plafond with Ankle Osteoarthritis

Yuya Oishi[1], Hiroaki Kurokawa[2], Shinichi Kosugi[3], Yasuhito Tanaka[2], Yuto Ishige[1], Masataka Yamamoto[1, 4], Hiroshi Takemura[1]

Tokyo University of Science, Department of Mechanical Engineering, Japan[1]
Email: 7520509@ed.tus.ac.jp

Nara Medical University, Japan[2]

Kosugi Orthopaedic & Rheumatology Clinic, Japan[3]

Hiroshima University, Japan[4]

Abstract: The etiology of ankle osteoarthritis is not enough elucidated, and similar to hip and knee osteoarthritis, the ankle osteoarthritis caused cartilage loss and pain in daily life. However, the ankle osteoarthritis has a worse prognosis than the hip or the knee osteoarthritis. Considering the ankle osteoarthritis skeletal structure is important in selecting the appropriate surgery for the patient. Selecting the appropriate surgery will lead to an improved prognosis. X-ray images and Computed Tomography (CT) scan images are usually used to classify ankle osteoarthritis, but the evaluation of 3D bone structure is difficult and the classification based on two-dimensional measurements of X-ray and CT images may vary among medical doctors. The purpose of this study is to investigate the three-dimensional geometric deformation characteristics of tibial plafond by using statistical analysis. Deformation characteristics were found in high severity ankle osteoarthritis compared with mild group. In particular, there was a statistically significant difference in the varus deformity of the articular facet of medial malleolus and tibial plafond between stage 3B and mild group ($p < 0.006$), and the hyperostosis of the medial malleolus between stage 4 and mild group ($p < 0.002$). These results suggest that patients with severe ankle osteoarthritis have common deformity characteristics in the tibial plafond. On the contrary, there was no significant difference in the deformity of the edge of anterior and posterior tibial plafond. Such phenomena suggest that the edge of anterior and posterior tibial plafond deforms regardless of ankle osteoarthritis. This study contributes to the scientific advancement of ankle osteoarthritis surgery.

Keywords: Ankle; Osteoarthritis; Tibial plafond

I. INTRODUCTION

About 15% of the world's adult population suffers from joint pain and disability due to osteoarthritis [3], and osteoarthritis of the foot accounts for about 1% of that [1]. Similar to osteoarthritis of the hip and knee, osteoarthritis of the ankle wears away cartilage and causes pain in daily life. However, the outcome and prognosis of ankle osteoarthritis are not as good as those of hip and knee osteoarthritis. In severe cases of ankle osteoarthritis, the bones start to collide with each other. Examining the bone shape of ankle osteoarthritis is important in choosing the right surgery for the patient. Choosing the right surgery can lead to a better prognosis. There is less clinical and basic research on ankle osteoarthritis than on hip and knee osteoarthritis. The etiology of primary ankle osteoarthritis is not fully understood [9]. Knowledge of the basic etiology is essential for the selection of appropriate surgery for ankle osteoarthritis [10]. Various analyses of ankle osteoarthritis have been performed based on data obtained from radiographic and CT images [5,9,12,13].

Corresponding Author: Hiroshi Takemura. Tokyo University of Science, Yamazaki 2641, Noda, Japan, Tel: 04-7124-1501 (3931), Fax: 04-7123-9814, E-mail: takemura@rs.tus.ac.jp

Ankle osteoarthritis has been classified into four levels and five stages in the Takakura-Tanaka classification system [4,7]. To classify ankle osteoarthritis in clinical practice, X-ray and CT images are usually used. However, two-dimensional analysis by the human eye has problems such as variability of results depending on the subjective criteria of the clinician. Regardless of the significance of three-dimensional analysis, there are few reports of three-dimensional analysis of tibial plafond in ankle osteoarthritis. Three-dimensional analysis studies of the articular surface of the tibiofemoral joint and the tibia have been developed [11,15]. Three-dimensional shape statistical analysis was applied to the osteoarthritic tibial plafond. Three-dimensional geometric analysis of the tibia has already been performed. However, it is limited to healthy subjects and the geometry is only localized. The tibial region needs to be elucidated gradually. In addition, it is important to investigate deformity features that are not caused by osteoarthritis to study ankle deformities. The purpose of this study was to investigate the three-dimensional geometric deformation characteristics of tibial plafond according to the classification of ankle osteoarthritis and the deformation characteristics independent of ankle osteoarthritis by statistical analysis.

II. DATA COLLECTION

A Study Population

The study population consisted of twelve ankle osteoarthritis patients (sex: female, 18 feet: 10 right, 8 left, age: 69.3 ± 6.5 years). All included patients had the Japan nationality. The ankle osteoarthritis patients were classified into four levels and five stages using Takakura and Tanaka classification [4,7]. Fig. 1 shows X-ray images of ankle osteoarthritis at each level and stage. Each level and stage of the classification were as follows:

stage 1: No joint-space narrowing, but early sclerosis and osteophyte formation.

stage 2: Narrowing of the joint space medially.

stage 3A: The obliteration of the joint space was limited to the medial malleolus.

stage 3B: The obliteration extended to the roof of the dome of the talus.

stage 4: The obliteration of the whole joint space with complete bone contact.

The number of the joints for patients at each stage was three joints in normal, one joint in stage 1, three joints in stage 2, two joints in stage 3A, four joints in stage 3B, and five joints in stage 4. In this study, the mild group consists of normal, stage 1, and stage 2.

We captured the CT images at the Heisei Memorial Hospital, which is a social medical corporation under the cooperation of the Nara Medical University. This study has been approved by the medical ethical committee of Nara Medical University.

B Scanning Condition

In this study, the foot images were captured using a CT scanner (Optimal CT 600, GE Healthcare Inc). The subjects were in the supine position during CT acquisition. In addition, a medical compressor (DynaWell® loading device) was used for the subjects assuming that ankle joint loading in stance position. The CT scan was performed using the compressor while axial loading 300 N. The imaging interval was 0.625 mm. The right foot images of each subject were assigned to the left foot images by reversing the right foot images of each subject concerning to the sagittal plane.

III. ANALYSIS METHODS

A. Three-Dimensional Bone Shape Model

The data obtained from the CT scanning was an X-ray image. The slice images were output in the format of a medical imaging standard called Digital Imaging and Communication in Medicine (DICOM). In this study, a resolution of 512 x 512 pixels and a density resolution of 16 bits were used for DICOM. Three-dimensional bone models were manually created from the DICOM data. ITK-SNAP allows the stacking of specified regions from the DICOM data to create 3D bone models in Stereolithography (STL) and Visualization Toolkit (VTK) format. The 3D bone model was created for each subject.

B. Quantification of Bone 3D Deformity

To quantify the bone deformation of each subject, the volume registration method was employed [6,8]. The volume registration method relates similar regions by calculating the deformation field that minimizes the luminance error between two volumes. We adopted the approach proposed by Szeliski and Coughlan [6]. The computed deformation field is represented by a three-dimensional grid. The deformation field consists of control points. Each control point had three degrees of freedom, consisting of three translations. The volume size of the image data used was 256 × 256 × 256 voxels, and the control points were placed at every 16 × 16 × 16

voxel vertex, so the number of control points was 4913 (17 × 17 × 17) and the total number of degrees of freedom was 14739. The displacement of the control points is a quantified value of the shape difference between the two volumes. Figure 2 shows the definition of the coordinate system in this study.

C. Principal Component Analysis

Principal Component Analysis (PCA) [2] was conducted on the values of the tibial plafond deformity characteristics quantified by the volume registration method. The PCA was used for dimensionality reduction, characteristic extraction, data compression, and representation of significant factors as principal components. The PCA transforms the variables that represent distinctive displacement field changes into principal components [14,16]. Each principal component visualizes the geometric changes in the tibial plafond.

Principal component scores were evaluated with Welch's t-test. The level of statistical significance was defined as $p < 0.01$.

IV. RESULTS

A. Principal Component Analysis Results

Figure 3 shows the distribution of principal components obtained by PCA on the displacement field of the tibia. The diagonal graph in Figure 3 shows the probability density of each principal component. To investigate the correlation between the principal components and the stage of osteoarthritis, Figure 3 shows the distribution of the principal components from the first to the sixth principal components. The weighting coefficients were set to $+2\sigma_i$ or $-2\sigma_i$ to emphasize the differences in deformation characteristics. σ_i is the standard deviation of the i-th principal component score.

B. Characteristics of 1st - 6th Principal Components

The features of tibia deformity represented by each principal component and the contribution rate of each principal component were as follows:

1st principal component
: Features: Z-axis rotation (+), flattening medial malleolus, the hyperostosis of the edge of tibial plafond, varus deformity of the articular facet of the medial malleolus. Contribution rate: 28.1%.

2nd principal component
: Features: Z-axis rotation (-), flattening medial malleolus, varus deformity of the articular facet of the medial malleolus. Contribution rate: 21.3%.

3rd principal component
: Features: sharping and extending medial malleolus, flattening posterior and anterior medial malleolus. Contribution rate: 9.8%.

4th principal component
: Features: the hyperostosis of the edge of anterior tibial plafond, translation of tibia plafond for lateral, flattening and the hyperostosis of anterior medial malleolus, the hyperostosis of posterior medial malleolus. Contribution rate: 9.7%.

5th principal component
: Features: Z-axis rotation (-) of the medial malleolus, the hyperostosis of anterior tibial plafond. Contribution rate: 6.4%.

6th principal component
: Features: the hyperostosis of the anterior medial malleolus, sharping posterior medial malleolus, the reduction of the edge of the tibial plafond. Contribution rate: 6.3%.

Some principal components have common features because each principal component has multiple deformities. For example, in Figure 4, one is $+2\sigma_1$ and the other is $+2\sigma_2$. In Figure 4, the anterior medial malleolus deformities are the same between the bones, but the other deformities of the bones are different from each other. In the first and second principal components, the anterior medial malleolus is indeed deformed. From Figure 5, they are $+2\sigma_1$ and $-2\sigma_1$, respectively. Thus, the anterior medial malleolus is a factor in the deformation of the 1st and 2nd principal components.

V. DISCUSSION

In the 2nd principal component, a statistically significant difference ($p<0.006$) was found between stage 3B and the mild disease group (Figure 6). Figure 7 shows the deformities of bone shape by the 2nd principal component. As the 2nd principal component increases, the part of the tibial plafond outlined in red in Figure 7 changes. This indicates that the tibial plafond is varus deformed and the medial malleolus is varus deformed. Tashiro et al. reported that the articular surface of the tibial plafond and articular surface of medial malleolus in ankle osteoarthritis groups was varus deformity [5]. Therefore, the present study is partially consistent with that report.

Furthermore, a statistically significant difference ($p < 0.002$) was found between stage 4 and mild groups (normal, stage 1, and stage 2) in the 4th principal

component (Figure 8). Figure 9 shows the deformation of bone shape by the 4th principal component. As the 4th principal component increases, the edge of the anterior tibial plafond declines, and the edge of the posterior tibial plafond increases.

In the 3rd principal component, there was no significant difference between normal subjects and stage 2, 3B, and 4 subjects (Figure 10). This suggests that the 3rd principal component is deformed regardless of ankle osteoarthritis stages. Figure 11 shows the tibial plafond deformities of the 3rd principal component change. As the 3rd principal component increases, the edge of the anterior and posterior tibial plafond shrinks as if the umbrella were shrinking. This suggests that the anterior-posterior deformation of the edge of the anterior and posterior tibial plafond is not caused by ankle osteoarthritis progression.

The limitation of this study is that the number of subjects is small. Stage 3A, which was particularly small in number but high in severity, is also likely to have a characteristic deformity. It is also necessary to identify the characteristics of early stages, such as stage 1 and stage 2, which were defined as mild in this study. Since ankle osteoarthritis is supposed to worsen in stages, it is possible that characteristically deformed in stages, either from the beginning or from the middle. In this experiment, Figure 3 did not show the clear relationship and consistent deformity between each stage of ankle osteoarthritis and principal components. However, this study suggests a clear relationship between the mild group and high severe patients which high severity ankle osteoarthritis has a characteristic deformity and that the tibial plafond has deformity characteristics not caused by ankle osteoarthritis.

VI. CONCLUSION

This study performed geometric shape statistical analysis by using PCA for the tibial plafond and the medial malleolus. The sum of the cumulative contribution rate of the sixth principal component is reached 80%. This study has not been raised concerning the consistent deformity between each stage of ankle osteoarthritis and principal components. However, three-dimensional bone shape structure features in stages 3B, and 4 were found in the 2nd and 4th principal components, respectively. Statistically significant differences were found in the varus deformity of the articular facet of the medial malleolus and tibial plafond between stage 3B and the mild group, and the hyperostosis of the edge of anterior tibial plafond and the medial malleolus between stage 4 and the mild group. The analytical results suggest that patients with high severity ankle osteoarthritis have tibial plafond common deformity characteristics and that the tibial plafond has deformity characteristics not caused by ankle osteoarthritis progression. This study contributes to revealing the tibial plafond deformity characteristics in ankle osteoarthritis, and to the clarification of the deformity characteristics of ankle osteoarthritis, which may lead to the elucidation of mechanism, surgery planning, and early diagnosis.

REFERENCES

[1] Peyron JG. The epidemiology of osteoarthritis. In: MoskowitzRW, Howell DS, Goldberg VM, Mankin HJ, eds.Osteoarthritis.Diagnosis and Treatment. Philadelphia, PA: WB Saunders; pp. 9–27, 1984.

[2] S. Wold, K. Esbensen and P. Geladi, "Principal Component Analysis", *Chemometrics and Intelligent Laboratory Systems*, Vol. 2, pp. 37–52, 1987.

[3] Felson DT. The epidemiology of osteoarthritis: prevalence andrisk factors. In: Kuettner KE, Goldberg VM, eds. Osteoarthritis Disorders. Rosemont, IL: American Academy of Orthopaedic Surgeons; pp. 13–24, 1995.

[4] Y. Takakura, Y. Tanaka, T. Kumai and S. Tamai, "Low Tibial Osteotomy for Osteoarthritis of the Ankle", *The Journal of Bone and Joint Surgery*, Vol. 77-B, No. 1, pp. 50–54, Jan. 1995.

[5] K. Tashiro, T. Teramoto, C. Miyamoto and R. Suzuki, "Radiological Assessment of the Osteoarthritic Ankle - Difference between Inversion and Eversion Type-", *Orthopedics & traumatology*, Vol. 47, No. 4, pp. 966–970, 1997.

[6] Szeliski, R. and Coughlan, J., "Spline-based image registration." *International Journal of Computer Vision*. Vol. 22, No. 3, pp. 199–218, 1997.

[7] M. Tada, H. Yoshida, M. Mochimaru, and T. Kanade, "Generating subject-specific FE models of fingertip with the use of MR volume registration.", In Proceedings of Eurohaptics. pp. 99–104, 2006.

[8] K. Hayashi, K. Tanaka, T. Kumai, K. Sugimoto, Y. Takakura, "Correlation of Compensatory Alignment of the Subtalar Joint to the Progression of Primary Osteoarthritis of the Ankle", *Foot and Ankle International*, Vol. 29, No. 4, pp. 400–406, April 2008.

[9] Y. Tanaka, Y. Takakura, K. Hayashi, A. Taniguchi, T. Kumai and K. Sugimoto, "Low tibial osteotomy for varus-type osteoarthritis of the ankle", *The Journal of Bone and Joint Surgery*, Vol. 88-B, No. 7, pp. 909–913, July 2006.

[10] Victor Valderrabano MD, PhD, Monika Horisberger MD, Iain Russell MD, Hugh Dougall MD and Beat Hintermann MD, Etiology of Ankle Osteoarthritis, *Clinical Orthopaedics and Related Research*, Vol. 467, No. 7, pp. 1800–1806, July 2009.

[11] Todd L. Bredbenner, Travis D. Eliason, Ryan S. Potter, Robert L. Mason, Lorena M. Havill, Daniel P. Nicolella, "Statistical shape modeling describes variation in tibia and femur surface geometry between Control and Incidence groups from the Osteoarthritis Initiative database", *Journal of Biomechanics*, Vol. 43, pp. 1780–1786, 2010.

[12] N. Holzery, D. Salvo, A.C.A. Marijnissen, K.L. Vincken, A.C. Ahmad, E. Serra, P. Hoffmeyer, R. Stern, A. Lübbeke, M. Assal, "Radiographic evaluation of posttraumatic osteoarthritis of the ankle: The Kellgren-Lawrence scale is reliable and correlates with clinical symptoms", *Osteoarthritis and Cartilage*, Vol. 23, pp. 363–369, 2015.

[13] Nicola Krähenbühla, Lena Sieglera, Manja Deforth, Lukas Zwicky, Beat Hintermann, Markus Knupp, "Subtalar joint alignment in ankle osteoarthritis", *Foot and Ankle Surgery*, Vol. 25, No. 2, pp. 143–149, April 2019.

[14] Takuya Fujinuma, Shinichi Kosugi, Hiroaki Kurokawa, Yasuhito Tanaka, Hiroshi Takemura and Satoki Tsuichihara, Evaluation of Tibiofibular Joint Alignment in Ankle Osteoarthritis Based on 3D Bone Thickness, *41st Annu. Int. Conf. of the IEEE Engineering in Medicine and Biology Society, EMBC 2019*, Berlin, pp.2123–2126, 2019.

[15] Liselore Quintens, Michiel Herteleer, sanne Vancleef, Yannick Carette, Joost Duflou, stefaan Nijs, Jos Vander sloten and Harm Hoekstra, "Anatomical Variation of the tibia – a principal Component Analysis", *Scientific Reports*, 9, 7649, 2019.

[16] T. Fujinuma, H. Takemura, S Kosugi, H. Kurokawa, Y Tanaka and S. Tsuichihara, Quantitative evaluation method for tibiofibular joint alignment in ankle osteoarthritis based on 3D bone size, *Journal of Musculoskeletal Research*, Vol. 23, No. 03, 2050011, 2020.

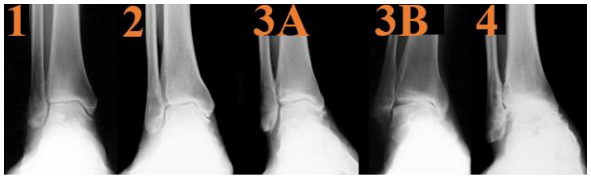

Fig. 1 ankle osteoarthritis classified into four levels and five stages. Orange characters are ankle osteoarthritis stages [4,7].

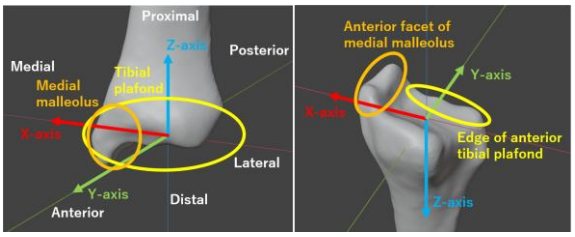

(a) From diagonally above (b) From the bottom

Fig. 2 Definition of the coordinate system. (a) and (b) are the distal part of the tibia. Medial malleolus and tibial plafond are in the red and yellow circle of (a), respectively. The articular facet of medial malleolus and edge of anterior tibial plafond are in red and yellow circle of (b), respectively. The red, green, and blue lines represent X-axis, Y-axis, and Z-axis respectively.
Origin: The intersection of the tibial plafond and Z-axis.
X-axis: Cross-product Y- and Z-axes.
Y-axis: The axis of the shaft of the second metatarsal.
Z-axis: The axis along the tibia length.

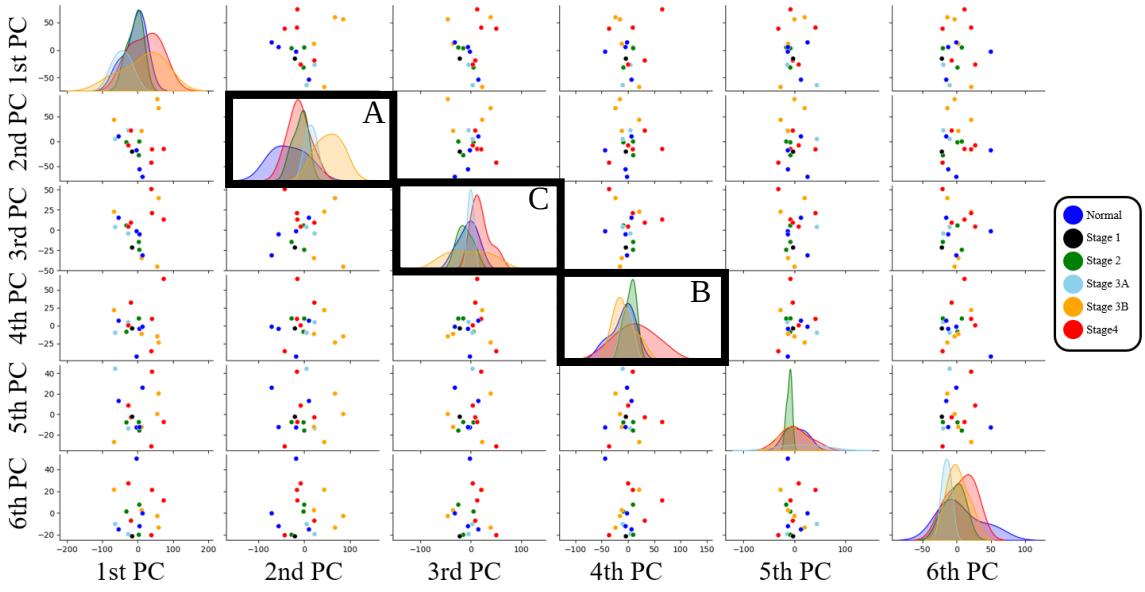

Fig. 3 1st-6th principal components score. PC is principal component. Each principal component was shared across the y-axes across a single row and the x-axes across a single column. The diagonal plots showed probability distributions in each principal component. A, B and C are one-dimensionalized and magnified in Fig. 6, Fig. 8 Fig. 10 respectively.

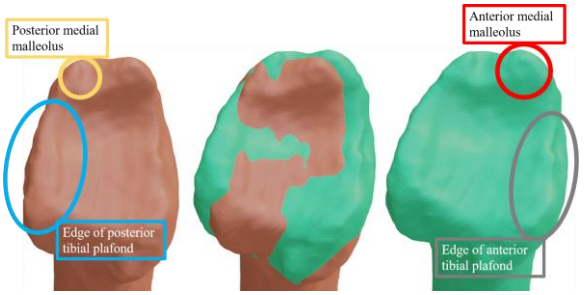

Fig. 4 Difference between $+2\sigma_1$ (green) and $-2\sigma_1$ (orange) in the average tibia. The green tibia is the average tibia added $+2\sigma_1$ and the orange tibia is the average tibia added $-2\sigma_1$.

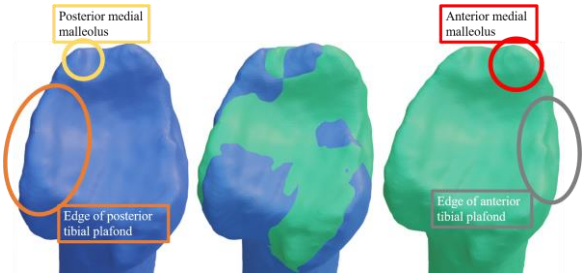

Fig. 5 Difference between $+2\sigma_1$ (green) and $+2\sigma_2$ (blue) in the average tibia. The green tibia is the average tibia added $+2\sigma_1$, and the blue tibia is the average tibia added $+2\sigma_2$.

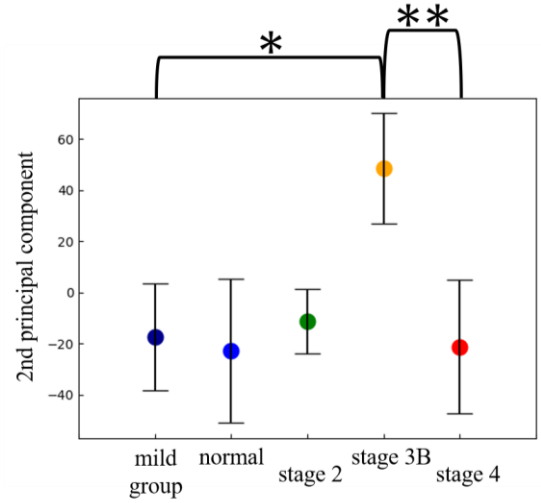

Fig. 6 2nd principal component score. * Indicates a significant difference ($p < 0.006$). ** Indicates a significant difference ($p < 0.007$).

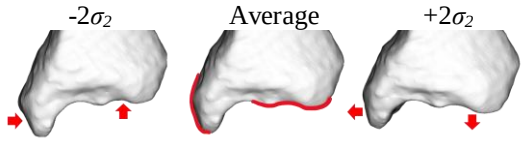

Fig. 7 Deformity of tibial plafond shape in 2nd principal component.

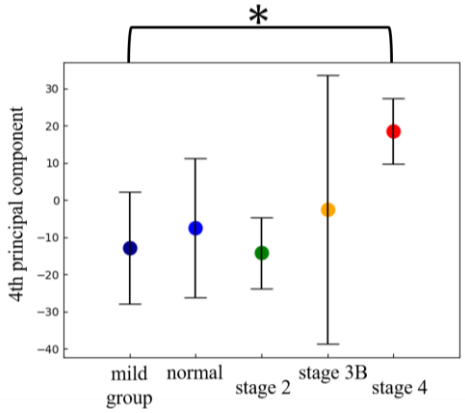

Fig. 8 4th principal component score. * Indicates a significant difference ($p < 0.002$).

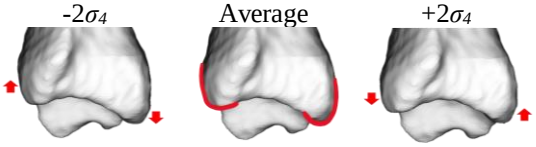

Fig. 9 Deformity of tibial plafond shape in 4th principal component.

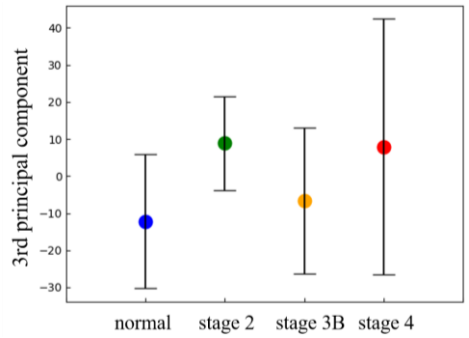

Fig. 10 4th principal component score. There was no significant difference among normal, stage 2, stage 3B, and stage 4 ($p > 0.05$).

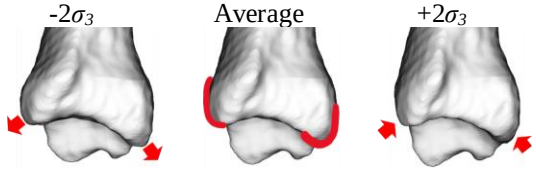

Fig.11 Deformity of tibial plafond shape in 3rd principal component.